BUCKLING ANALYSIS OF THIN-WALLED SECTIONS UNDER LOCALISED LOADING USING THE SEMI-ANALYTICAL FINITE STRIP METHOD

GREGORY J. HANCOCK
CAO HUNG PHAM

RESEARCH REPORT R951
JUNE 2014

ISSN 1833-2781

SCHOOL OF CIVIL ENGINEERING

THE UNIVERSITY OF SYDNEY

THE UNIVERSITY OF SYDNEY

SCHOOL OF CIVIL ENGINEERING

BUCKLING ANALYSIS OF THIN-WALLED SECTIONS UNDER LOCALISED LOADING USING THE SEMI-ANALYTICAL FINITE STRIP METHOD

RESEARCH REPORT R951

GREGORY J. HANCOCK
CAO HUNG PHAM

June 2014

ISSN 1833-2781

Copyright Notice

School of Civil Engineering, Research Report R951
Buckling Analysis of Thin-Walled Sections under Localised Loading
using the Semi-Analytical Finite Strip Method

Gregory J. Hancock
Cao Hung Pham

June 2014

ISSN 1833-2781

Published by:
School of Civil Engineering
The University of Sydney
Sydney NSW 2006
Australia

This report and other Research Reports published by the School of Civil Engineering are available at http://sydney.edu.au/civil

ABSTRACT

Thin-walled sections under localised loading may lead to web crippling of the sections. This report develops the Semi-Analytical Finite Strip Method (SAFSM) for thin-walled sections subject to localised loading to investigate web crippling phenomena. The method is benchmarked against analytical solutions, Finite Element Method (FEM) solutions, as well as Spline Finite Strip Method (SFSM) solutions.

The report summarises the SAFSM theory then applies it to the buckling of plates, and channel sections under localised loading. Multiple series terms in the longitudinal direction are used to compute the pre-buckling stresses in the plates and sections, and to perform the buckling analyses using these stresses. Solution convergence with increasing numbers of series terms is provided in the report. The more localised the loading and buckling mode, the more series terms are required for accurate solutions.

KEYWORDS

Thin-walled sections; Localised loading; Buckling analysis; Semi-analytical finite strip method; Spline finite strip method.

TABLE OF CONTENTS

INTRODUCTION

Thin-walled sections and plates under localised loading leading to plate buckling have been studied analytically for a long period mainly as part of investigations of web plates of sections at points of concentrated load. Two of the most comprehensive summaries of the work to date have been by Khan and Walker (1972) where the buckling of plates subject to localised loading was investigated and Johansson and Lagerqwist (1995) where the resistance of plate edges to localised loading is summarised. More recently, Natario, Silvestre and Camotim (2012) have further developed these investigations for beams subjected to concentrated loads using Generalised Beam Theory (GBT). They benchmark GBT for plates, un-lipped channels and I-sections against the earlier research and the Shell Finite Element method (SFE). To date, the Finite Strip Method (FSM) of analysis developed by YK Cheung (1976) does not appear to have been used for buckling studies under localised loading. As the FSM is used extensively in the Direct Strength Method (DSM) of design of cold-formed sections in the North American Specification NAS S100 (AISI, 2012) and the Australian/New Zealand Standard AS/NZS 4600 (Standards Australia, 2005) it is important that the FSM of buckling analysis is extended to localised loading. This report further develops the Semi-Analytical Finite Strip Method (SAFSM) for thin-walled sections subject to localised loading and benchmarks it against the Spline Finite Strip Method (SFSM) used previously by Pham and Hancock (2009, 2012) for shear buckling problems and the Finite Element Method program-ABAQUS/Standard (2008) version 6.8-2.

Folded plate and finite strip theories for the buckling analysis of thin-walled sections and stiffened panels in longitudinal and transverse compression and shear have been developed since the mid-1960s. Two basic approaches were adopted. These are the exact solutions of Wittrick (1968), and Williams and Wittrick (1969), and the approximate solutions of Przemieniecki (1972) and Plank and Wittrick (1974) based on the finite strip method of analysis developed by YK Cheung (1976). Most of this research was applied to aeronautical structures where the longitudinal and transverse compression as well as shear is assumed constant as in the stiffened panels of aeroplane wings. Recently, Chu et al (2005) and Bui (2009) have applied the SAFSM to the buckling of thin-walled sections under more general loading conditions so that multiple series terms are used to capture the modulation of the buckles that occur. These latter papers are restricted to bending of the sections and transverse compression and shear are not included. The application of the SAFSM to uniform shear of thin-walled sections has recently been applied by Hancock and Pham (2013) where multiple series terms in the longitudinal direction are used to perform the buckling analyses. In the present report, the method in Hancock and Pham (2013) is extended to include the potential energy resulting from varying longitudinal, transverse and shear stresses. Multiple series terms in the longitudinal direction are used to compute the pre-buckling stresses in the plates and sections, and to perform the buckling analyses using these stresses. Solution convergence with increasing numbers of series terms is provided. The more localised the loading and hence buckling mode, the more series terms are required for accurate solutions especially for longer sections with concentrated loads.

FINITE STRIP PRE-BUCKLING AND BUCKLING ANALYSES

The finite strip method developed by YK Cheung (1976) is similar to the finite element method in that approximate displacement functions are used to represent the plate flexural and membrane deformations. The theorem of minimum total potential energy is applied to compute the resulting stiffness equations. The SAFSM allows the deformations and stresses to be computed for any folded plate system satisfying the boundary conditions assumed. Normally, the sections are assumed simply supported at the ends so that the harmonic functions in the longitudinal direction are orthogonal thus allowing the different series terms to be uncoupled in the linear stiffness analysis. This produces considerable computational advantages for the SAFSM compared with the FEM. Longitudinal functions for other boundary conditions can be chosen which are also orthogonal as given by Cheung (1976). The resulting stiffness equations are summarised by:

$$[K]\{\delta\} = \{W\} \tag{1}$$

where [K] is the system stiffness matrix based on a strip subdivision of a thin-walled section as shown in Fig. 1, {δ} are the nodal line displacements of the strips in the global X,Y,Z axes, and {W} are the nodal line forces (line loads) as also shown in Fig. 1. [K] is based on the strain energy of the strip elements, and {W} is based on the potential energy of the line loads.

Equation 1 can be solved for the nodal line displacements {δ} in the global X,Y,Z axes, and the flexural and membrane stresses {σ} in the strips. These are pre-buckling displacements and stresses and are also described by harmonic functions.

Based on the pre-buckling membrane stresses {σ}, the stability equations given by Equation 2 can be derived from the minimum total potential of the system undergoing buckling deformations. Since the buckling deformations also satisfy the simply supported boundary conditions, the same displacement functions are used for the buckling deformations as for the pre-buckling deformations.

$$([K] - \lambda[G])\{\delta\} = 0 \tag{2}$$

where [G] is the system stability matrix and λ is the load factor against buckling. The report concentrates the development of the stability matrix [G] for strips under generalised membrane stresses resulting from line loading as shown in Fig. 1. The formulation of the stiffness matrix [K] was given previously in detail in Cheung (1976).

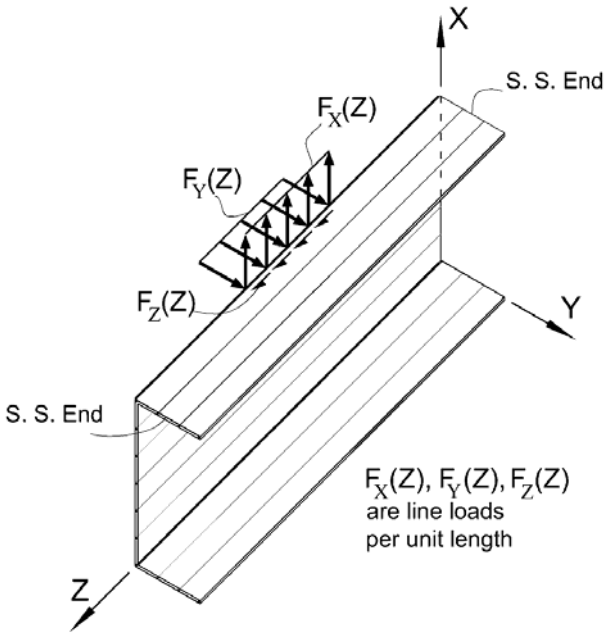

Figure 1. Line Loads on Channel Section showing Global Axes X,Y,Z

PLATE DEFORMATIONS

The plate flexural deformations (w) of a strip can be described by the summation over μ series terms as:

$$w = \sum_{m=1}^{\mu} f_{1m}(y).X_{1m}(x) \tag{3}$$

where the x-axis is in the longitudinal direction in the plane of the strip, the y-axis is in the transverse direction in the plane of the strip, and w is in the z-direction perpendicular to the strip as shown in Fig. 2.

The function $f_{1m}(y)$ for the mth series term is the transverse variation given by:

$$f_{1m}(y) = \alpha_{1Fm} + \alpha_{2Fm}.\left(\frac{y}{b}\right) + \alpha_{3Fm}.\left(\frac{y}{b}\right)^2 + \alpha_{4Fm}.\left(\frac{y}{b}\right)^3 \tag{4}$$

where the 4 polynomial coefficients α_{iFm} for the mth series term depend on the nodal line deformations of the strip. The term b is the width of the strip.

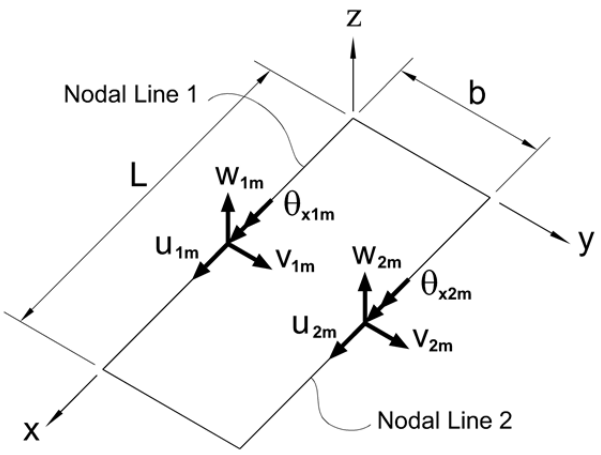

Figure 2. Strip Local Axes x,y,z and Nodal Line Deformations for the mth series term

The function $X_{1m}(x)$ is the longitudinal variation of the mth series term and is given by:

$$X_{1m}(x) = sin\left(\frac{m\pi x}{L}\right) \tag{5}$$

where L is the length of the strip. The function $X_{1m}(x)$ satisfies the simply supported boundary conditions assumed in this report. Other boundary conditions can be used in the SAFSM as set out in Cheung (1976) but are not considered in this report.

The plate membrane deformations (u, v) in the (x,y) directions respectively can be described by the summation over μ series terms as:

$$v = \sum_{m=1}^{\mu} f_{vm}(y).X_{1m}(x) \tag{6}$$

$$u = \sum_{m=1}^{\mu} f_{um}(y).X'_{1m}(x).\frac{L}{m\pi} \tag{7}$$

The functions $f_{um}(y)$ and $f_{vm}(y)$ are the transverse variations given by:

$$f_{vm}(y) = \alpha_{1Mm} + \alpha_{2Mm}.\left(\frac{y}{b}\right) \tag{8}$$

$$f_{um}(y) = \alpha_{3Mm} + \alpha_{4Mm}.\left(\frac{y}{b}\right) \tag{9}$$

where the 4 polynomial coefficients α_{iMm} for the mth series term depend on the nodal line deformations of the strip.

The nodal line flexural deformations $\{\delta_{Fm}\} = (w_{1m}, \theta_{x1m}, w_{2m}, \theta_{x2m})^T$ in Fig. 2 can be related to the polynomial coefficients in (4) above by:

$$\{\delta_{Fm}\} = [C_F]\{\alpha_{Fm}\} \tag{10}$$

where $\{\alpha_{Fm}\} = (\alpha_{1Fm} \quad \alpha_{2Fm} \quad \alpha_{3Fm} \quad \alpha_{4Fm})^T$

Similarly, the nodal line membrane deformations $\{\delta_{Mm}\} = (u_{1m}, v_{1m}, u_{2m}, v_{2m})^T$ in Fig. 2 can be related to the polynomial coefficients in (8) and (9) above by:

$$\{\delta_{Mm}\} = [C_M]\{\alpha_{Mm}\} \tag{11}$$

where $\{\alpha_{Mm}\} = (\alpha_{1Mm} \quad \alpha_{2Mm} \quad \alpha_{3Mm} \quad \alpha_{4Mm})^T$

The matrices $[C_F]$ and $[C_M]$ have inverses $[C_F]^{-1}$, $[C_M]^{-1}$ which are given in Appendices 1 and 2 respectively. The resulting equations for the plate flexural and membrane deformations are given by:

$$w = \sum_{m=1}^{\mu} X_{1m}[\Gamma_{FL}][C_F]^{-1}\{\delta_{Fm}\} \tag{12}$$

where $$[\Gamma_{FL}] = [1 \quad (y/b) \quad (y/b)^2 \quad (y/b)^3\,] \tag{13}$$

$$u = \sum_{m=1}^{\mu} X'_{1m}.\frac{L}{m\pi}[\Gamma_{Mu}][C_M]^{-1}\{\delta_{Mm}\} \tag{14}$$

where $$[\Gamma_{Mu}] = [0 \quad 0 \quad 1\,(y/b)] \tag{15}$$

$$v = \sum_{m=1}^{\mu} X_{1m}[\Gamma_{Mv}][C_M]^{-1}\{\delta_{Mm}\} \tag{16}$$

where $$[\Gamma_{Mv}] = [1 \quad (y/b) \quad 0 \;\; 0\,] \tag{17}$$

In the computation of the potential energy described later, derivatives of the plate flexural and membrane deformations are required. The derivatives used are as follows:

$$\frac{\partial w}{\partial x} = \sum_{m=1}^{\mu}[\Gamma_{FL}]\,X'_{1m}\{\alpha_{Fm}\} \tag{18}$$

$$\frac{\partial w}{\partial y} = \sum_{m=1}^{\mu}\frac{1}{b}[\Gamma_{FT}]\,X_{1m}\{\alpha_{Fm}\} \tag{19}$$

where $$[\Gamma_{FT}] = [0 \quad 1 \quad 2(y/b) \quad 3(y/b)^2\,] \tag{20}$$

$$\frac{\partial u}{\partial x} = \sum_{m=1}^{\mu} X''_{1m}.\frac{L}{m\pi}[\Gamma_{Mu}]\,\{\alpha_{Mm}\} \tag{21}$$

$$\frac{\partial v}{\partial x} = \sum_{m=1}^{\mu} X'_{1m}[\Gamma_{Mv}]\,\{\alpha_{Mm}\} \tag{22}$$

PLATE THEORY AND MEMBRANE STRESSES

The plate flexural theory is that used by Cheung (1976) and is given by:

$$\{M\} = [D_F]\{\kappa\} \tag{23}$$

where

$$[D_F] = \begin{bmatrix} D & \nu D & 0 \\ \nu D & D & 0 \\ 0 & 0 & \frac{D(1-\nu)}{2} \end{bmatrix} \tag{24}$$

$$\{M\} = (M_x \quad M_y \quad M_{xy})^T \tag{25}$$

$$\{\kappa\} = \left(-\frac{\partial^2 w}{\partial x^2} \quad -\frac{\partial^2 w}{\partial y^2} \quad 2\frac{\partial^2 w}{\partial x \partial y}\right)^T \tag{26}$$

with the plate flexural rigidity $D = Et^3/12(1-\nu^2)$, where E is the Young's modulus, and v is the Poisson's ratio. The plate membrane theory is that used by Cheung (1976) and is given by:

$$\{\sigma\} = [D_M]\{\varepsilon\} \tag{27}$$

$$[D_M] = \begin{bmatrix} E_1 & \nu E_1 & 0 \\ \nu E_1 & E_1 & 0 \\ 0 & 0 & G \end{bmatrix} \tag{28}$$

$$\{\sigma\} = (\sigma_x \quad \sigma_y \quad \tau_{xy})^T \tag{29}$$

$$\{\varepsilon\} = \left[\frac{\partial u}{\partial x} \quad \frac{\partial v}{\partial y} \quad \frac{\partial u}{\partial y} + \frac{\partial v}{\partial x}\right]^T \tag{30}$$

with the plate membrane rigidity $E_1 = E/(1-v^2)$, where G is the shear modulus = E/2(1+v).

Substitution for v from (16) and u from (14) in (30) allows the membrane stresses to be computed from the nodal line deformations using (27). The full matrix for computing the membrane stresses is given in Appendix 3. Note that the normal stresses vary as the sine function whereas the shear stresses vary as the cosine function.

STRAIN ENERGY AND POTENTIAL ENERGY

In order to compute the stiffness and stability matrices of the strip according to conventional finite strip theory (Cheung, 1976), it is necessary to define the strain energy in the strip under deformation and the potential energy of the membrane forces.

The flexural strain energy U_F is given by:

$$U_F = \frac{1}{2}\int_0^L \int_0^b (-M_x \frac{\partial^2 w}{\partial x^2} - M_y \frac{\partial^2 w}{\partial y^2} + 2M_{xy} \frac{\partial^2 w}{\partial x \partial y})\, dy\, dx \tag{31}$$

The membrane strain energy U_M is given by:

$$U_M = \frac{1}{2}\int_0^L \int_0^b (\sigma_x \varepsilon_x + \sigma_y \varepsilon_y + \tau_{xy}\gamma_{xy})\, dy\, dx \tag{32}$$

The flexural potential energy of the membrane forces V_F is given by:

$$V_F = -\frac{1}{2}\int_0^L \int_0^b (\sigma_x(x).\left(\frac{\partial w}{\partial x}\right)^2 + \sigma_y(x).\left(\frac{\partial w}{\partial y}\right)^2 + 2\tau_{xy}(x)\left(\frac{\partial w}{\partial x}\right)\left(\frac{\partial w}{\partial y}\right))\, t dy\, dx \tag{33}$$

where $\sigma_x(x)$, $\sigma_y(x)$, and $\tau_{xy}(x)$ are the assumed membrane normal and shear stresses with the signs given in Fig. 3, and t is the plate thickness.

The membrane stresses are derived from the finite strip pre-buckling linear elastic analysis of the plate assembly subjected to partial line loads located along the nodal lines as shown in Fig. 1. Equation 1 is used to determine the pre-buckling nodal line deformations, so that the stresses can be computed as described in the previous section. The transverse stress and shear stress in a strip are each assumed uniform across the strip width and computed from the means on the two nodal lines. The resulting membrane stresses can be described by harmonic functions in the longitudinal direction and linear or constant functions in the transverse direction as follows:

$$\sigma_x(x) = \left(\sigma_1(x) + \left(\sigma_2(x) - \sigma_1(x)\right).\left(\frac{y}{b}\right)\right) = \sum_{k=1}^{\mu} \sigma_k(x).(\sigma_{1k} + (\sigma_{2k} - \sigma_{1k}).\left(\frac{y}{b}\right)) \tag{34}$$

where $\sigma_k(x) = \sin\left(\frac{k\pi x}{L}\right)$ (35)

$$\sigma_y(x) = \sum_{k=1}^{\mu} \sigma_k(x).(\sigma_{Tk}) \tag{36}$$

$$\tau_{xy}(x) = \sum_{k=1}^{\mu} \tau_k(x).(\tau_k) \tag{37}$$

where $\tau_k(x) = \cos\left(\frac{k\pi x}{L}\right)$ (38)

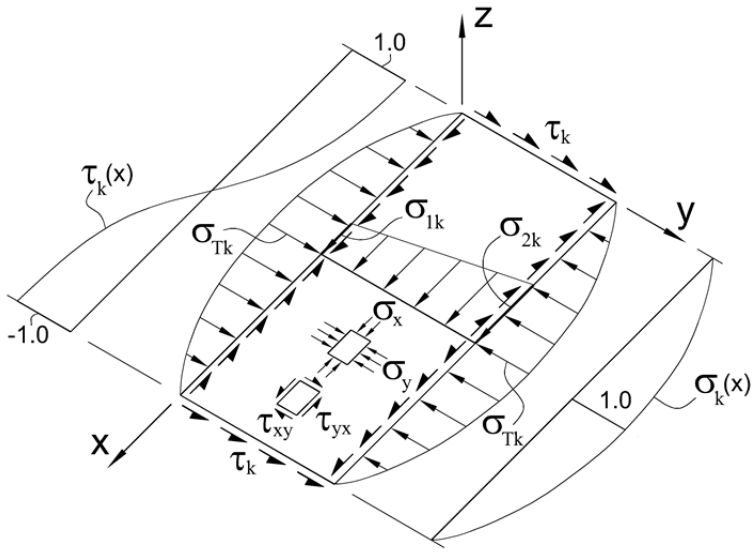

Figure 3. Assumed Membrane Stresses (k = 1)

Substitution of Equations 34, 36 and 37 in Equation 33 using Equations 18 and 19 results in

$$V_F = V_{FL} + V_{FT} + V_{FS1} + V_{FS2} \tag{39}$$

where

$$V_{FL} = -\frac{1}{2}\int_0^L\int_0^b \sum_{m=1}^{\mu}\sum_{n=1}^{\mu}\{\alpha_{Fm}\}^T[\Gamma_{FL}]^T X'_{1m}\sum_{k=1}^{\mu}\sigma_k(x).(\sigma_{1k} + (\sigma_{2k} - \sigma_{1k}).\left(\frac{y}{b}\right))[\Gamma_{FL}]X'_{1n}\{\alpha_{Fn}\}tdxdy \tag{40}$$

$$V_{FT} = -\frac{1}{2}\int_0^L\int_0^b \sum_{m=1}^{\mu}\sum_{n=1}^{\mu}\{\alpha_{Fm}\}^T[\Gamma_{FT}]^T \frac{1}{b}X_{1m}\sum_{k=1}^{\mu}\sigma_k(x).(\sigma_{Tk})[\Gamma_{FT}]\frac{1}{b}X_{1n}\{\alpha_{Fn}\}tdydx \tag{41}$$

$$V_{FS1} = -\frac{1}{2}\int_0^L\int_0^b \sum_{m=1}^{\mu}\sum_{n=1}^{\mu}\{\alpha_{Fm}\}^T[\Gamma_{FL}]^T X'_{1m}\sum_{k=1}^{\mu}\tau_k(x).(\tau_k)[\Gamma_{FT}]\frac{1}{b}X_{1n}\{\alpha_{Fn}\}tdydx \tag{42}$$

$$V_{FS2} = -\frac{1}{2}\int_0^L\int_0^b \sum_{m=1}^{\mu}\sum_{n=1}^{\mu}\{\alpha_{Fm}\}^T[\Gamma_{FT}]^T \frac{1}{b}X_{1m}\sum_{k=1}^{\mu}\tau_k(x).(\tau_k)[\Gamma_{FL}]X'_{1n}\{\alpha_{Fn}\}tdydx \tag{43}$$

The membrane potential energy of the membrane forces V_M is given by:

$$V_M = -\frac{1}{2}\int_0^L\int_0^b(\sigma_x(x)\left(\frac{\partial u}{\partial x}\right)^2 + \sigma_x(x)\left(\frac{\partial v}{\partial x}\right)^2)\,tdy\,dx \tag{44}$$

As stated in Plank and Wittrick (1974), it is believed that there are no membrane instabilities associated with transverse stress and shear stress so that there are no terms in Equation 44 associated with these.

Substitution of Equation 34 in Equation 44 using Equations 21 and 22 results in

$$V_M = V_{Mu} + V_{Mv} \tag{45}$$

where

$$V_{Mu} = -\frac{1}{2}\int_0^L\int_0^b \sum_{m=1}^{\mu}\sum_{n=1}^{\mu}\{\alpha_{Mm}\}^T[\Gamma_{Mu}]^T X''_{1m}\frac{L}{m\pi}\sum_{k=1}^{\mu}\sigma_k(x).(\sigma_{1k} + (\sigma_{2k} - \sigma_{1k}).\left(\frac{y}{b}\right))[\Gamma_{Mu}]X''_{1n}\frac{L}{n\pi}\{\alpha_{Mn}\}tdydx \tag{46}$$

$$V_{Mv} = -\frac{1}{2}\int_0^L\int_0^b \sum_{m=1}^{\mu}\sum_{n=1}^{\mu}\{\alpha_{Mm}\}^T[\Gamma_{Mv}]^T X'_{1m}\sum_{k=1}^{\mu}\sigma_k(x).(\sigma_{1k} + (\sigma_{2k} - \sigma_{1k}).\left(\frac{y}{b}\right))[\Gamma_{Mv}]X'_{1n}\{\alpha_{Mn}\}tdydx \tag{47}$$

STIFFNESS AND STABILITY MATRICES

For equilibrium, the theorem of minimum total potential energy of the flexural energy with respect to each of the elements $\{\delta_{Fm}\}$ is:

$$\frac{\partial(U_F+V_F)}{\partial\{\delta_{Fm}\}} = 0 \tag{48}$$

The result is:

$$[k_{Fm}]\{\delta_{Fm}\} + \sum_{n=1}^{\mu}[g_{Fmn}]\{\delta_{Fn}\} = 0 \quad m = 1, 2, \ldots, \mu \tag{49}$$

The matrices $[k_{Fm}]$ and $[g_{Fmn}]$ are given in Appendix 1. The coefficients C_{Lwmnk} , C_{Tmnk} , C_{S1mnk} , C_{S2mnk} in Appendix 1 have been evaluated exactly for the harmonic functions satisfying the simply supported boundary conditions. They can be evaluated for other harmonic functions satisfying other boundary conditions as explained by Cheung (1976).

For equilibrium, the theorem of minimum total potential for the membrane energy is:

$$\frac{\partial(U_M+V_M)}{\partial\{\delta_{Mm}\}} = 0 \tag{50}$$

The result is:

$$[k_{Mm}]\{\delta_{Mm}\} + \sum_{n=1}^{\mu}[g_{Mmn}]\{\delta_{Mn}\} = 0 \quad m = 1, 2, \ldots, \mu \tag{51}$$

The matrices $[k_{Mm}]$ and $[g_{Mmn}]$ are given in Appendix 2. The coefficients C_{Lumnk} , C_{Lvmnk} in Appendix 2 have been evaluated exactly for the harmonic functions satisfying the simply supported boundary conditions. They can be evaluated for other harmonic functions satisfying other boundary conditions as explained by Cheung (1976).

For folded plate assemblies including thin-walled sections such as channels, (49) and (51) must be transformed to a global co-ordinate system to assemble the stiffness $[K_m]$ and stability $[G_m]$ matrices of the folded plate assembly or section. Since the flexural displacements w given by (3) and the membrane displacements v given by (6) use the same longitudinal displacement function $X_{1m}(x)$, they are conformable resulting in convergence to classical solutions for thin-walled sections.

The buckling equations for a folded plate system derived from (49) and (51) are given by (2) and require eigenvalue routines to determine the buckling load factors λ:

EIGENVALUE AND EIGENVECTOR ROUTINES

A computer program **bfinst10.cpp** has been written in Visual Studio C++ to assemble the stiffness equations and stability equations to solve for the pre-buckling displacements and pre-buckling stresses using equations 1 and 27, then buckling load factors (eigenvalues) and buckling modes (eigenvectors) using Equations 2, 49 and 51. The eigenvalues are computed using the Sturm sequence property described by Turnbull (1946) and Peters and Wilkinson (1969), and the corresponding eigenvectors using the method as described by Wilkinson (1958).

The matrix [G] has 4 * N * μ degrees of freedom where N is the number of nodal lines and μ is the number of series terms. If the rows and columns in the matrix [G] are organised so that each degree of freedom is taken over the μ series terms, then the half-bandwidth of the matrix is simply μ times the half-bandwidth of the problem with one series term. This speeds the computation of the eigenvalues and eigenvectors considerably.

SOLUTIONS TO PLATES AND SECTIONS WITH LOCALISED LOADING AT CENTRE

PLATE SIMPLY SUPPORTED ON ALL FOUR EDGES

The solutions for a plate of length L simply supported along all four edges determined using the bfinst10.cpp analysis is compared with the solution based on the equation of Johansson and Lagerqvist (1995), the Spline Finite Strip Method (SFSM) (Pham and Hancock 2009) and the Finite Element Method program-ABAQUS/Standard (2008) version 6.8-2. The equation for the elastic buckling of a rectangular plate is given as:

$$\sigma_{cr} = \frac{k\,\pi^2 E}{12(1-\nu^2)\,(h/t)^2} \Big/ \left(\frac{n}{h}\right) \qquad (52)$$

where n is the length of the loaded portion subject to the stress σ_{cr}, h is the depth of the plate which may consist of multiple strips and k is the plate buckling coefficient for transverse compression.

The analysis is carried out for 8 equal width strips and an increasing number of series terms. Load length ratios (n/L) of 0.025, 0.05, 0.200 and 0.250 and aspect ratios (h/L) of 1:1, 1:2, 1:5 and 1:10 have been investigated and the solutions for the buckling coefficient k are compared in Table 1 with those of Johansson and Lagerqvist (1995), the SFSM where 8 strips and 80 splines have been used, and the FEM where 5mm square elements have been used. It is clear that the SAFSM solutions become more accurate with increasing numbers of series terms, and that more terms are required for higher aspect ratios and lower load length ratios. The solutions converge to values slightly higher than those of the SFSM and FEM. Five series terms seem adequate for square plates and plates with an aspect ratio of 2.0. However, for higher aspect ratios such as L/h = 5.0, at least 11 series terms are necessary and 19 series terms are needed to achieve accuracies better than 2% when the load length ratio n/L = 0.05. This is a fairly concentrated load on a longer length. For an aspect ratio of 10, an accuracy better than 3% is achieved with 25 series terms. It is interesting to note that the equation of Johansson and Lagerqvist (1995) is not accurate for aspect ratios of 5.0 and 10.0.

Load length ratio (n/L)	Aspect ratio (L/h)	Johansson and Lagerqvist (1995)	SFSM	FEM (ABAQUS)	SAFSM (bfinst10.cpp) (series terms in brackets)
0.250	1.0	3.450	3.383	3.399	3.480 (5) 3.478 (11)
0.050	2.0	2.409	2.360	2.368	2.421(5) 2.404(11) 2.404(15)
0.200	2.0	2.544	2.508	2.515	2.549 (5) 2.545 (11)
0.050	5.0	2.178	1.983	1.991	2.066 (11) 2.018 (19)
0.200	5.0	2.628	2.582	2.590	2.697 (7) 2.597 (11)
0.025	10.0	2.138	1.392	1.392	1.433 (25)

Table 1. Buckling coefficients k for simply supported rectangular plates under localised load along one longitudinal edge at the centre of the plate

The buckling mode for an aspect ratio (L/h) of 5:1, a load length ratio (n/L) of 0.20 and 11 series terms determined from bfinst10.cpp is plotted in Fig. 4. The buckling mode has one localised buckle at the centre with the buckle located slightly towards the loaded edge.

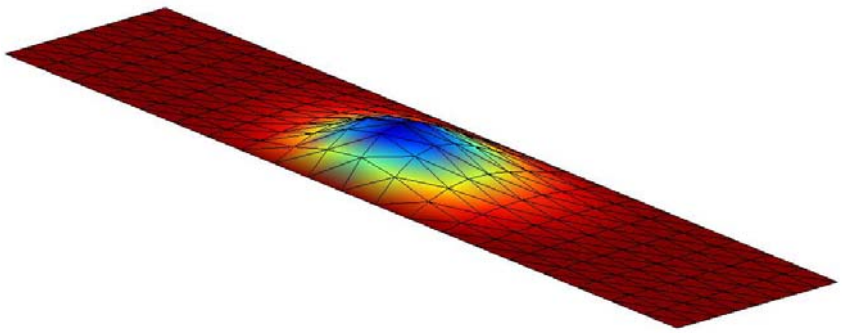

Figure 4. Rectangular Plate Buckling Mode Single Edge Loading L/h = 5.0, n/h = 1.0

UNLIPPED CHANNEL SECTION UNDER LOCALISED LOADING

In order to extend the study to unlipped channel sections, a 250 mm deep overall unlipped channel with overall flange width 90 mm, thickness 6 mm as tested by Young and Hancock (2001) has been used. The section contains rounded corners with an internal radius of 7.9 mm. The strip subdivision used is 4, 8, 4 strips for each of the flanges, the web and each of the corners respectively making 24 strips in total with 25 nodal lines. The number of degrees of freedom of the unconstrained section is therefore 100 for each series term considered. For example, when 11 series terms are used, the number of degrees of freedom is 1100, and the half-bandwidth is 8 for each series term times 11 series terms making 88. This section has also been studied by Natario et al (2012) using Generalised Beam Theory (GBT).

In this report, two loading cases have been studied. The first is the Interior One Flange (IOF) loading case with a length between supports of 933 mm which the specimen length of 1023 mm reported by Young and Hancock (2001) less half the bearing length of n = 90 mm at each end support. The second is the Interior Two Flange (ITF) loading case with a length of 838 mm also reported by Young and Hancock (2001). The line loading applied is assumed along a length n = 90 mm at the centre and located at the junction of the corner and top flange for IOF, and at the junctions of the corner and top and bottom flanges for ITF. These nodal lines are also assumed to be prevented against lateral deflection in the direction perpendicular to the web. The loads at buckling are given in Table 2.

Loading Case	Length (mm) Loading Length (mm)	SFSM Web only simply supported	SFSM Web, flange and lip simply supported	FEM (ABAQUS) Web only simply supported	FEM (ABAQUS) Web, flange and lip simply supported	SAFSM (bfinst10.cpp) (series terms in brackets)
IOF	933 90	438.35	438.37	455.36	455.40	464.3 (11) 463.5 (15)
ITF	838 90	295.35	299.78	299.22	302.28	304.12 (11) 304.10 (15)

Table 2. Unlipped Channel Buckling Loads in kN

Two different sets of boundary conditions have been used for comparison. These are the web only simply supported as in the tests of Young and Hancock, and the web, flange and lip simply supported (i.e. no buckling deformation in plane of cross section at the ends but free to deform longitudinally). The latter boundary conditions are the same as assumed in the SAFSM analysis with the simply supported harmonic functions. The SAFSM (bfinst10.cpp) solution with 11 series terms appears accurate for both loading cases and both sets of boundary conditions with the maximum error better than 2% compared with the FEM. The solutions are close to the GBT solutions of Natario et al (2012) for the ITF case (291 kN) but lower for the IOF case (494 kN). The IOF problem seems to be very sensitive to small changes in boundary conditions and restraints assumed. The GBT solution assumed lateral restraint at the loading point alone.

The buckling modes for the IOF and ITF cases are given in Figs. 5 and 6 respectively.

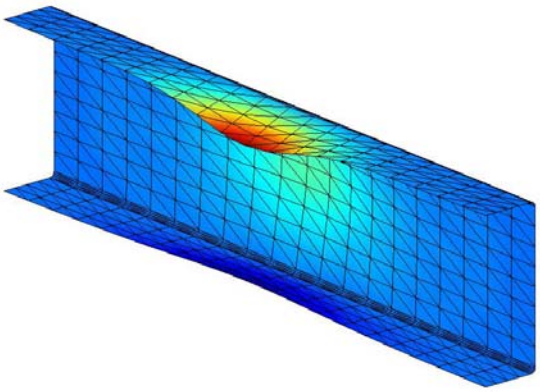

Figure 5. Unlipped Channel IOF Loading Case n = 90 mm, L = 933 mm

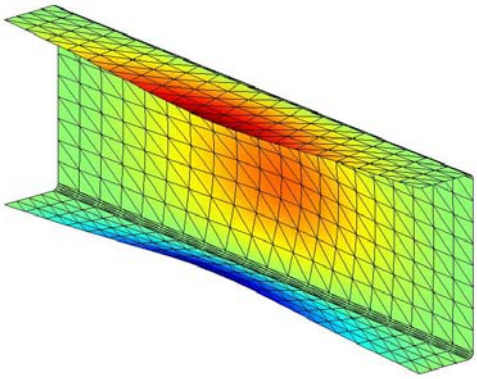

Figure 6. Unlipped Channel ITF Loading Case n = 90 mm, L = 838 mm

LIPPED CHANNEL SECTION UNDER LOCALISED LOADING

A 200 mm deep lipped channel with flange width 80mm, lip length 20 mm as studied by Pham and Hancock (2009) and Hancock and Pham (2013) has been investigated. These dimensions are all centreline and not overall. In Pham and Hancock (2009, 2012), the section studied was 2 mm thick. This has been reduced to 1 mm to match with the 200 mm deep plate simply supported on all four edges in the previous section. Further, the section now contains rounded corners with an internal radius of 5 mm. The strip subdivision used is 1, 4, 8, 4 strips for each of the lips, flanges, the web and each of the corners respectively making 34 strips in total with 35 nodal lines. The length is 1000 mm and the loading applied is along a length n = 200 mm or n = 50 mm at the centre and located at the junction of the corner and top flange for IOF loading and also at the junction of the corner and bottom flange for ITF loading. These nodal lines are also assumed to be prevented against lateral deflection in the direction perpendicular to the web and load. Two different sets of boundary conditions have been used in the FEM analysis for comparison. These are the web only simply supported (SS), and the web, flange and lip simply supported (i.e. no buckling deformation in the plane of the

cross section at the ends but free to deform longitudinally). The latter boundary conditions are the same as assumed in the SAFSM analysis with the simply supported harmonic functions.

The buckling loads are given in kN in Table 3. The SAFSM solutions are close to the FEM web, flange and lip simply supported cases as would be expected since these are the boundary conditions assumed for the simply supported boundary conditions of all strips. The buckling coefficients according to Eq. 52 are also given in Table 2 and can be compared with those in Table 1. The buckling coefficients are more than 2.5 times those for the simple plate in Table 1. The SAFSM (bfinst10.cpp) solutions with 7 series terms are accurate to better than 0.2% when compared with the FEM solutions for both the IOF and ITF loading cases when n/L = 0.20 (200mm case). They are accurate to better than 1.0% with 15 series terms when n/L = 0.05 (50mm case).

Loading Case	**Length (mm)** **Load length (mm)**	**FEM (ABAQUS)** **Web only SS**	**FEM (ABAQUS)** **Web, flange and lip SS**	**SAFSM (bfinst10)** **(series terms in brackets)**	**Buckling Coefficient in Eq. 52** **k**
IOF	1000 200	5.410	6.009	6.024 (7) 6.017 (11) 6.016 (15)	6.665 (7) 6.657 (11) 6.656 (15)
ITF	1000 200	2.731	3.056	3.051 (7) 3.049 (11) 3.049 (15)	3.375 (7) 3.374 (11) 3.374 (15)
IOF	1000 50	4.766	5.175	5.303 (7) 5.234 (11) 5.221 (15)	5.867 (7) 5.791 (11) 5.778 (15)
ITF	1000 50	2.472	2.727	2.746 (7) 2.737 (11) 2.735 (15)	3.039 (7) 3.028 (11) 3.026 (15)

Table 3. Lipped channel buckling loads in kN and coefficients k

The buckling mode for the IOF case with L= 1000 mm and n = 200 mm is shown in Fig. 7.

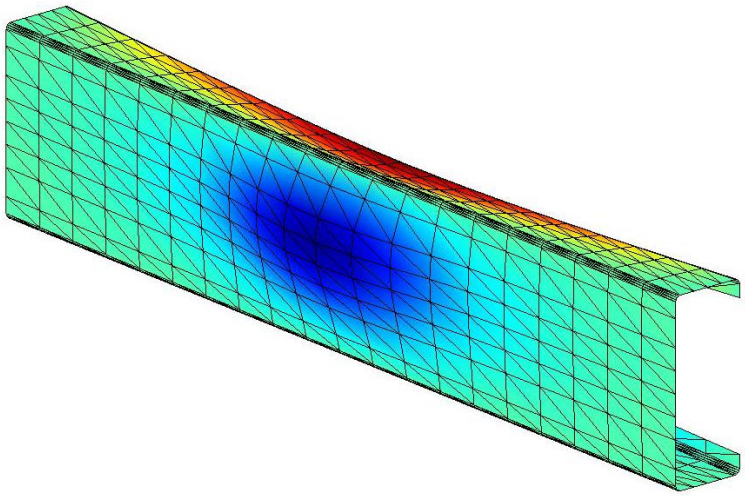

Figure 7. Lipped Channel with IOF Central Load at Flange/Corner Junction n = 200mm, L = 1000mm

WEB-STIFFENED CHANNEL UNDER LOCALISED LOADING

A 200 mm deep lipped channel with flange width 80 mm, lip length 20 mm, web stiffener with a rectangular indent of 5 mm over a depth of 80 mm located symmetrically about the centre of the web, as studied by Pham and Hancock (2009) and Hancock and Pham (2013) has been investigated. These dimensions are all centreline and not overall. In Hancock and Pham (2013), the section studied was 2 mm thick. This has been reduced to 1 mm to match with the 200 mm deep plate simply supported on all four edges in the previous section. The section now contains rounded corners with an internal radius of 5 mm. The strip subdivision used is 1, 4, 4, 1, 4 strips for each of the lips, flanges, the web flats, web stiffeners and each of the corners respectively making 40 strips in total with 41 nodal lines. The SAFSM (bfinst10.cpp) solutions shown in Table 3 with 25 series terms produce an accuracy better than 2.0% when compared with the FEM solutions for the IOF loading case when n/L = 0.05 (50 mm case) and the flange, web and lip are simply supported. Localisation of the buckle in the flange as shown in Fig. 8 requires more series terms than for the simple lipped channel shown in Fig. 7 where localization does not occur. The buckling coefficients k for the IOF case are more than four times those for the simply supported plate in Table 4.

Loading Case	Length (mm) Loading Length (mm)	FEM (ABAQUS) Web only SS	FEM (ABAQUS) Web, flange and lip SS	SAFSM (bfinst10.cpp) (series terms in brackets)	Buckling Coefficient in Eq. 52 k
IOF	1000 50	6.725	7.894	8.526 (7) 8.421 (15) 8.212 (21) 8.063 (25)	9.432 (7) 9.317 (15) 9.085 (21) 8.921 (25)
ITF	1000 50	4.152	5.417	5.482 (7) 5.480 (11) 5.475 (15)	6.066 (7) 6.062 (11) 6.058 (15)

Table 4. Web-stiffened channel buckling loads in kN and coefficients k

The loads for the case of web only simply supported computed using the FEM are considerably lower than the flange, web and lip simply supported case and demonstrate that this problem is more sensitive to the end boundary conditions than the simple lipped channel. Alternative orthogonal functions $X_{1m}(x)$ according to Cheung (1976) are under investigation for this case and other boundary conditions such as the end one flange EOF and end two flange ETF loading cases.

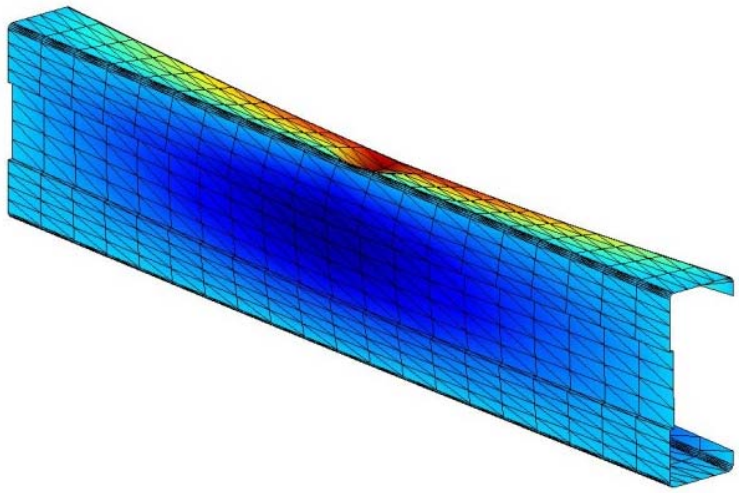

Figure 8. Web-Stiffened Channel with IOF Central Load at Flange/Corner Junction n = 50 mm, L = 1000 mm

Buckling modes for two different ITF cases are shown in Figs. 9 and 10. No flange localisation occurs in these cases and so less series terms are required as shown in Table 4.

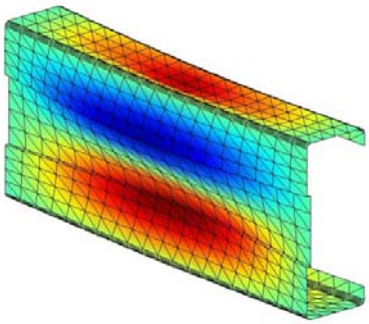

Figure 9. Web-Stiffened Channel with ITF Central Load at Flange/Corner Junction n = 50 mm, L = 500 mm

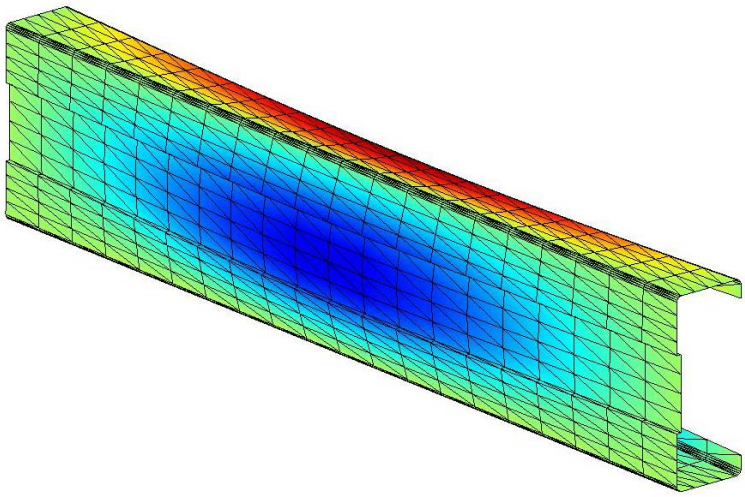

Figure 10. Web-Stiffened Channel with ITF Central Load at Flange/Corner Junction n = 50 mm, L = 1000 mm

CONCLUSION

A semi-analytical finite strip method (SAFSM) buckling analysis of thin-walled section subjected to localised loading has been developed and benchmarked against spline finite strip method (SFSM) and finite element method (FEM) solutions.

The method has proven to be accurate and efficient compared with the SFSM and FEM methods. The more localised the load, and the longer the section under load then the greater the number of series terms required.

ACKNOWLEDGEMENT

Funding provided by the Australian Research Council Discovery Project Grant DP110103948 has been used to perform this project. The SFSM program used was developed by Gabriele Eccher and the graphics program was developed by Song Hong Pham.

REFERENCES

ABAQUS/Standard Version 6.8-2; ABAQUS/CAE User's Manual. (2008), Dassault Systèmes Simulia Corp., Providence, RI, USA.

American Iron and Steel Institute (AISI) (2012), "North American Specification for the Design of Cold-Formed Steel Structural Members." 2012 Edition, AISI S100-2012.

Bui, H.C. (2009), "Buckling Analysis of Thin-Walled Sections under General Loading Conditions", Thin-Walled Structures, Vol. 47, pp 730-739.

Cheung, Y.K. (1976), Finite Strip Method in Structural Analysis, Pergamon Press, Inc. New York, N.Y.

Chu, X.T, Ye, Z.M., Kettle, R.,Li, L.Y. (2005), "Buckling Behaviour of Cold-Formed Channel Sections under Uniformly Distributed Loads", Thin-Walled Structures, Vol. 43, pp 531-542.

Hancock, G.J. and Pham, C.H. (2013), "Shear Buckling of Channel Sections with Simply Supported Ends using the Semi-Analytical Finite Strip Method", Thin-Walled Structures, Vol. 71, pp 72-80.

Johansson, B.J. and Lagerqvist, O. (1995), "Resistance of Plate Edges to Concentrated Forces", Journal of Constructional Steel Research, Vol 32, pp 69-105.

Khan, M.Z. and Walker, A.C. (1972), "Buckling of Plates subjected to Localised Edge Loading", The Structural Engineer, Vol 50, No. 6 (June), pp 225-232.

Natario, P, Silvestre, N. and Camotim, D. (2012), "Localized Web Buckling Analysis of Beams subjected to Concentrated Loads using GBT", Thin-Walled Structures, Vol. 61, pp 27-41.

Pham, C. H., and Hancock, G. J. (2009). "Shear Buckling of Thin-Walled Channel Sections." Journal of Constructional Steel Research, Vol. 65, No. 3, pp. 578-585.

Pham, C. H., and Hancock, G. J. (2012). "Elastic Buckling of Cold-Formed Channel Sections in Shear." *Thin-*Walled Structures, Vol. 61, pp. 22-26.

Peters, G. And Wilkinson, J.H. (1969), "Eigenvalues of Ax = λBx with Band Symmetric A and B", Computer Journal, Vol. 12, pp 398-404.

Plank, R. J., and Wittrick, W. H. (1974), "Buckling Under Combined Loading of Thin, Flat-Walled Structures by a Complex Finite Strip Method", International Journal for Numerical Methods in Engineering, Vol. 8, No. 2, pp 323-329.

Przmieniecki, J. S .D. (1973), "Finite Element Structural Analysis of Local Instability", Journal of the American Institute of Aeronautics and Astronautics, Vol. 11, No. 1.

Standards Australia. (2005). "AS/NZS 4600:2005, Cold-Formed Steel Structures." Standards Australia/ Standards New Zealand.

Turnbull, H. W. (1946), Theory of Equations, Oliver and Boyd, Edinburgh and London.

Wilkinson, J. H. (1958), "The calculation of the eigenvectors of co-diagonal matrices", Computer Journal, Vol. 1, pp 90-96.

Wittrick, W. H. (1968), "A unified approach to the initial buckling of stiffened panels in compression", Aeronautical Quarterly, 19, 265-283.

Williams, F.W. and Wittrick, W.H.(1969), "Computational procedures for a matrix analysis of the stability and vibration of thin flat-walled structures in compression", Int. Journal of Mechanical Sciences, 11, 979-998.

Young, B., and Hancock, G. J. (2001). "Design of Cold-Formed Channels." *Journal of Structural Engineering, ASCE*, Vol. 127, No. 10, pp. 1137-1144.

APPENDIX 1: FLEXURAL STIFFNESS AND STABILITY MATRICES

$$[k_{Fm}] = [C_F]^{-T}\,[k_{\alpha Fm}]\,[C_F]^{-1} \tag{A1-1}$$

$$[g_{Fmn}] = [C_F]^{-T}\,[g_{\alpha FLmn} + g_{\alpha FTmn} + g_{\alpha FS1mn} + g_{\alpha FS2mn}]\,[C_F]^{-1} \tag{A1-2}$$

where

$$[C_F]^{-1} = \begin{bmatrix} 1 & 0 & 0 & 0 \\ 0 & b & 0 & 0 \\ -3 & -2b & 3 & -b \\ 2 & b & -2 & b \end{bmatrix}$$

$[k_{\alpha Fm}]$ =

$$\begin{bmatrix} \left(\frac{DX}{2}\right) & \left(\frac{DX}{4}\right) & \left(\frac{DX}{6} - D1\right) & \left(\frac{DX}{8} - \frac{3D1}{2}\right) \\ \left(\frac{DX}{4}\right) & \left(\frac{DX}{6} + 2DXY\right) & \left(\frac{DX}{8} - \frac{D1}{2} + 2DXY\right) & \left(\frac{DX}{10} - D1 + 2DXY\right) \\ \left(\frac{DX}{6} - D1\right) & \left(\frac{DX}{8} - \frac{D1}{2} + 2DXY\right) & \left(\frac{DX}{10} - \frac{2D1}{3} + 2DY + \frac{8DXY}{3}\right) & \left(\frac{DX}{12} - D1 + 3DY + 3DXY\right) \\ \left(\frac{DX}{8} - \frac{3D1}{2}\right) & \left(\frac{DX}{10} - D1 + 2DXY\right) & \left(\frac{DX}{12} - D1 + 3DY + 3DXY\right) & \left(\frac{DX}{14} - \frac{6D1}{5} + 6DY + \frac{18DXY}{5}\right) \end{bmatrix}$$

where

$$DX = D\left(\frac{m\pi}{L}\right)^4 A$$

$$DY = \frac{D}{b^4}\,A$$

$$D1 = \nu\, D\left(\frac{m\pi}{bL}\right)^2 A$$

$$DXY = \frac{G\,t^3}{12}\left(\frac{m\pi}{bL}\right)^2 A$$

$$A = b\,L$$

$$D = \frac{E\,t^3}{12\,(1 - \nu^2)}$$

$$[g_{\alpha FLmn}] = \frac{2mn}{\pi}\sum_{k=1}^{\mu} C_{Lwmnk}\begin{bmatrix} \left(f_{1k}+\frac{f_{2k}}{2}\right) & \left(\frac{f_{1k}}{2}+\frac{f_{2k}}{3}\right) & \left(\frac{f_{1k}}{3}+\frac{f_{2k}}{4}\right) & \left(\frac{f_{1k}}{4}+\frac{f_{2k}}{5}\right) \\ \left(\frac{f_{1k}}{2}+\frac{f_{2k}}{3}\right) & \left(\frac{f_{1k}}{3}+\frac{f_{2k}}{4}\right) & \left(\frac{f_{1k}}{4}+\frac{f_{2k}}{5}\right) & \left(\frac{f_{1k}}{5}+\frac{f_{2k}}{6}\right) \\ \left(\frac{f_{1k}}{3}+\frac{f_{2k}}{4}\right) & \left(\frac{f_{1k}}{4}+\frac{f_{2k}}{5}\right) & \left(\frac{f_{1k}}{5}+\frac{f_{2k}}{6}\right) & \left(\frac{f_{1k}}{6}+\frac{f_{2k}}{7}\right) \\ \left(\frac{f_{1k}}{4}+\frac{f_{2k}}{5}\right) & \left(\frac{f_{1k}}{5}+\frac{f_{2k}}{6}\right) & \left(\frac{f_{1k}}{6}+\frac{f_{2k}}{7}\right) & \left(\frac{f_{1k}}{7}+\frac{f_{2k}}{8}\right) \end{bmatrix}$$

$$[g_{\alpha FTmn}] = \frac{2}{\pi}\sum_{k=1}^{\mu} C_{Tmnk}\begin{bmatrix} 0 & 0 & 0 & 0 \\ 0 & (f_{3k}) & (f_{3k}) & (f_{3k}) \\ 0 & (f_{3k}) & \left(\frac{4f_{3k}}{3}\right) & \left(\frac{6f_{3k}}{4}\right) \\ 0 & (f_{3k}) & \left(\frac{6f_{3k}}{4}\right) & \left(\frac{9f_{3k}}{5}\right) \end{bmatrix}$$

$$[g_{\alpha FS1mn}] = \frac{2m}{\pi}\sum_{k=1}^{\mu} C_{S1mnk}\begin{bmatrix} 0 & f_{4k} & f_{4k} & f_{4k} \\ 0 & \frac{f_{4k}}{2} & \frac{2f_{4k}}{3} & \frac{3f_{4k}}{4} \\ 0 & \frac{f_{4k}}{3} & \frac{2f_{4k}}{4} & \frac{3f_{4}}{5} \\ 0 & \frac{f_{4}}{4} & \frac{2f_{4}}{5} & \frac{3f_{4}}{6} \end{bmatrix}$$

$$[g_{\alpha FS2mn}] = \frac{2n}{\pi}\sum_{k=1}^{\mu} C_{S2mnk}\begin{bmatrix} 0 & 0 & 0 & 0 \\ f_{4k} & \frac{f_{4k}}{2} & \frac{f_{4k}}{3} & \frac{f_{4k}}{4} \\ f_{4k} & \frac{2f_{4k}}{3} & \frac{2f_{4k}}{4} & \frac{2f_{4k}}{5} \\ f_{4k} & \frac{3f_{4k}}{4} & \frac{3f_{4k}}{5} & \frac{3f_{4k}}{6} \end{bmatrix}$$

where

$$f_{1k} = \left(\frac{\pi}{L}\right)^2 \frac{V}{2}\,\sigma_{1k}$$

$$f_{2k} = \left(\frac{\pi}{L}\right)^2 \frac{V}{2}\,(\sigma_{2k} - \sigma_{1k})$$

$$f_{3k} = \left(\frac{1}{b}\right)^2 \frac{V}{2}\,\sigma_{Tk}$$

$$f_{4k} = \left(\frac{\pi}{bL}\right) \frac{V}{2}\,\tau_{k}$$

$$V = b\,t\,L$$

$$C_{Lwmnk} = \int_{\xi=0}^{\pi} \sin k\xi \cos m\xi \cos n\xi \; d\xi = \left[-\frac{cos\lambda_1\xi}{\lambda_1} + \frac{cos\lambda_2\xi}{\lambda_2} - \frac{cos\lambda_3\xi}{\lambda_3} - \frac{cos\lambda_4\xi}{\lambda_4}\right]_{\xi=0}^{\xi=\pi}$$

where

$$\lambda_1 = k + m + n$$

$$\lambda_2 = -k + m + n$$

$$\lambda_3 = k - m + n$$

$$\lambda_4 = k + m - n$$

$$C_{Tmnk} = \int_{\xi=0}^{\pi} \sin k\xi \sin m\xi \sin n\xi \, d\xi = \left[\frac{cos\lambda_1\xi}{\lambda_1} - \frac{cos\lambda_2\xi}{\lambda_2} - \frac{cos\lambda_3\xi}{\lambda_3} - \frac{cos\lambda_4\xi}{\lambda_4}\right]_{\xi=0}^{\xi=\pi}$$

where

$$\lambda_1 = k + m + n$$

$$\lambda_2 = -k + m + n$$

$$\lambda_3 = k - m + n$$

$$\lambda_4 = k + m - n$$

$$C_{S1mnk} = \int_{\xi=0}^{\pi} \sin n\xi \cos k\xi \cos m\xi \, d\xi = \left[-\frac{cos\lambda_1\xi}{\lambda_1} + \frac{cos\lambda_2\xi}{\lambda_2} - \frac{cos\lambda_3\xi}{\lambda_3} - \frac{cos\lambda_4\xi}{\lambda_4}\right]_{\xi=0}^{\xi=\pi}$$

where

$$\lambda_1 = k + m + n$$

$$\lambda_2 = k + m - n$$

$$\lambda_3 = -k + m + n$$

$$\lambda_4 = k - m + n$$

$$C_{S2mnk} = \int_{\xi=0}^{\pi} \sin m\xi \cos k\xi \cos n\xi \, d\xi = \left[-\frac{cos\lambda_1\xi}{\lambda_1} + \frac{cos\lambda_2\xi}{\lambda_2} - \frac{cos\lambda_3\xi}{\lambda_3} - \frac{cos\lambda_4\xi}{\lambda_4}\right]_{\xi=0}^{\xi=\pi}$$

where

$$\lambda_1 = k + m + n$$

$$\lambda_2 = -k + m + n$$

$$\lambda_3 = k - m + n$$

$$\lambda_4 = k + m - n$$

The stresses σ_{1k}, σ_{2k}, σ_{Tk} and τ_k are shown in Fig. 3. It can be demonstrated mathematically that C_{Lwmnk}, C_{Tmnk}, C_{S1mnk}, C_{S2mnk} are all zero when λ_2, λ_3 or λ_4 are zero.

APPENDIX 2: MEMBRANE STIFFNESS AND STABILITY MATRICES

$$[k_{Mm}] = [C_M]^{-T} [k_{\alpha Mm}] [C_M]^{-1} \quad \text{(A2-1)}$$

$$[g_{Mmn}] = [C_M]^{-T} [g_{\alpha Mu} + g_{\alpha Mv}] [C_M]^{-1} \quad \text{(A2-2)}$$

where

$$[C_M]^{-1} = \begin{bmatrix} 0 & 1 & 0 & 0 \\ 0 & -1 & 0 & 1 \\ 1 & 0 & 0 & 0 \\ -1 & 0 & 1 & 0 \end{bmatrix}$$

$[k_{\alpha Mm}]$ =

$$\begin{bmatrix} \left(\frac{G1}{2}\right) & \left(\frac{G1}{4}\right) & 0 & \left(\frac{G1}{2bk}\right) \\ \left(\frac{G1}{4}\right) & \left(\frac{G1}{6}+\frac{E1}{2}\right) & \left(\frac{-E12}{2}\right) & \left(\frac{G1}{4bk}-\frac{E12}{4}\right) \\ 0 & \left(\frac{-E12}{2}\right) & \left(\frac{E2}{2}\right) & \left(\frac{E2}{4}\right) \\ \left(\frac{G1}{2bk}\right) & \left(\frac{G1}{4bk}-\frac{E12}{4}\right) & \left(\frac{E2}{4}\right) & \left(\frac{G1}{2(bk)^2}+\frac{E2}{6}\right) \end{bmatrix}$$

where

$$G1 = G\left(\frac{m\pi}{L}\right)^2 V$$

$$E1 = \frac{E_1}{b^2} V$$

$$E2 = E_1 \left(\frac{m\pi}{L}\right)^2 V$$

$$E12 = \nu E_1 \left(\frac{m\pi}{bL}\right) V$$

$$V = b\, t\, L$$

$$k = \frac{m\pi}{L}$$

$$E_1 = \frac{E}{(1-\nu^2)}$$

$$[g_{\alpha Mv}] = \frac{2mn}{\pi}\sum_{k=1}^{\mu} C_{Lvmnk}\begin{bmatrix} \left(f_{1k}+\frac{f_{2k}}{2}\right) & \left(\frac{f_{1k}}{2}+\frac{f_{2k}}{3}\right) & 0 & & 0 \\ \left(\frac{f_{1k}}{2}+\frac{f_{2k}}{3}\right) & \left(\frac{f_{1k}}{3}+\frac{f_{2k}}{4}\right) & 0 & & 0 \\ 0 & 0 & & 0 & 0 \\ 0 & 0 & & 0 & 0 \end{bmatrix}$$

$$[g_{\alpha Mu}] = \frac{2mn}{\pi}\sum_{k=1}^{\mu} C_{Lumnk}\begin{bmatrix} 0 & 0 & & 0 & 0 \\ 0 & 0 & & 0 & 0 \\ 0 & & 0 & \left(f_{1k}+\frac{f_{2k}}{2}\right) & \left(\frac{f_{1k}}{2}+\frac{f_{2k}}{3}\right) \\ 0 & & 0 & \left(\frac{f_{1k}}{2}+\frac{f_{2k}}{3}\right) & \left(\frac{f_{1k}}{3}+\frac{f_{2k}}{4}\right) \end{bmatrix}$$

where

$$f_{1k} = \left(\frac{\pi}{L}\right)^2 \frac{V}{2}\,\sigma_{1k}$$

$$f_{2k} = \left(\frac{\pi}{L}\right)^2 \frac{V}{2}\,(\sigma_{2k} - \sigma_{1k})$$

$$V = b\,t\,L$$

$$C_{Lumnk} = \int_{\xi=0}^{\pi} \sin k\xi \sin m\xi \sin n\xi \; d\xi = C_{Tmnk}$$

$$C_{Lvmnk} = \int_{\xi=0}^{\pi} \sin k\xi \cos m\xi \cos n\xi \; d\xi = C_{Lwmnk}$$

APPENDIX 3: MEMBRANE STRESSES

The membrane stresses can be evaluated for the kth harmonic from the nodal line displacements as follows

$$\begin{bmatrix}\sigma_{xk}\\ \sigma_{yk}\\ \tau_{xyk}\end{bmatrix}=\begin{bmatrix} 0 & \left(\frac{\upsilon E_1}{b}\right)\sin\left(\frac{k\pi x}{L}\right) & -E_1\left(\frac{k\pi}{L}\right)\sin\left(\frac{k\pi x}{L}\right) & -E_1\left(\frac{k\pi}{L}\right)\left(\frac{y}{b}\right)\sin\left(\frac{k\pi x}{L}\right)\\ 0 & \left(\frac{E_1}{b}\right)\sin\left(\frac{k\pi x}{L}\right) & -\nu E_1\left(\frac{k\pi}{L}\right)\sin\left(\frac{k\pi x}{L}\right) & -\nu E_1\left(\frac{k\pi}{L}\right)\left(\frac{y}{b}\right)\sin\left(\frac{k\pi x}{L}\right)\\ G\left(\frac{k\pi}{L}\right)\cos\left(\frac{k\pi x}{L}\right) & G\left(\frac{k\pi}{L}\right)\left(\frac{y}{b}\right)\cos\left(\frac{k\pi x}{L}\right) & 0 & \frac{G}{b}\cos\left(\frac{k\pi x}{L}\right)\end{bmatrix}\begin{bmatrix}\alpha'_{1k}\\ \alpha'_{2k}\\ \alpha'_{3k}\\ \alpha'_{4k}\end{bmatrix}$$